International Journal of Applied Engineering Research ISSN 0973-4562 Volume 12, Number 22 (2017) pp. 12102-12107

A Vibrational Energy Harvesting Interface Circuit with Maximum Power Point Tracking Control

Chong-Gun Yu
Professor, Department of Electronics Engineering, Incheon National University,
119 Academy-ro, Yeonsu-gu, Incheon, KS006, Republic of Korea.

Orcid: 0000-0003-0802-0113

Abstract

In this paper a CMOS interface circuit with MPPT (Maximum Power Point Tracking) control is presented for vibrational energy harvesting applications. In the proposed system a PMU (Power Management Unit) is employed at the output of a DC-DC boost converter to provide a regulated output with low-cost and simple architecture. In addition, an MPPT controller using FOC (Fractional Open Circuit) technique is designed to harvest maximum power from vibration devices and increase efficiency of overall system. The AC signal from vibration devices is converted into a DC signal by an AC-DC converter, and then boosted through the DC-DC boost converter. The boosted signal is converted into a duty-cycled and regulated signal and delivered to loads by the PMU. A full-wave rectifier using active diodes is used as the AC-DC converter for high efficiency, and a DC-DC boost converter architecture using a schottky diode is employed for a simple control circuitry. The proposed circuit has been designed in a 0.35-μm CMOS process, and the designed chip occupies 915 μm × 895 μm. Simulation results shows that the maximum end-to-end power efficiency of the entire circuit is 83.4%.

Keywords: Energy Harvesting, Vibrational Energy, MPPT, AC-DC Converter, DC-DC Converter, PMU.

INTRODUCTION

Recently, there has been much interest on energy harvesting technology that harvests energy from surrounding environment and drives small electronic devices [1-10]. Among the various energy sources used in energy harvesting, light energy is most widely used because of its high power conversion efficiency and easy accessibility. However, PV (photovoltaic) cells must be located outside the system in order to receive light. In addition, the area of the PV cell must be large to harvest a large amount of energy, which makes it difficult to apply the energy harvester to miniaturized and embedded systems. On the other hand, vibrational energy harvesting technology does not need to be exposed to the outside, so it is advantageous to apply to an embedded or inserted device. Therefore, it can be applied to a self-power generation system for very small sensor nodes such as an aircraft sensor, a personal healthcare monitoring system, and an environmental monitoring system.

Vibrational energy can be converted to electrical energy using piezoelectric (PZT) devices. Since the output signal of a PZT device is of an ac-type signal, an AC-DC converter is required to convert it into a dc-type signal. The signal rectified by the AC-DC converter is converted to a suitable form through a DC-DC converter, which is a power converter, and supplied to a load. In order for the harvested vibration energy to be efficiently transferred to the load, the power conversion efficiency of the AC-DC converter and the DC-DC converter must be high.

An energy conversion device has an MPP (Maximum Power Point) that outputs the maximum available power. MPPT (Maximum Power Point Tracking) is required because the MPP changes in real time due to changes in the surrounding environment. Among various techniques for MPPT, the hill-climbing method and the fractional open-circuit (FOC) method have been commonly used for energy harvesting systems. In the hill-climbing [1], the instantaneous output power is usually computed using a microcontroller, making this approach be unsuitable for micro-scale energy harvesting. The FOC method [3], [5] is based on the empirical observation that the MPP voltage of an energy conversion device is a fraction of its open circuit voltage. In this method, the MPP voltage is computed by sensing its open circuit voltage.

Among the vibrational energy harvesting papers with FOC-based MPPT, reference [3] shows that the maximum efficiency of the MPPT control block is as high as 98%, but only the MPPT control block is implemented without a power converter. Reference [5] shows that the maximum efficiency of a DC-DC converter is 80% but not the end-to-end efficiency. In addition, the output is an unregulated signal and has a disadvantage that the chip area is very large, which is 5.52 mm^2. Reference [6] implements a circuit with a relatively small size and has a regulated output signal. However, since MPPT control is not implemented, the overall efficiency is as low as about 60%. In this paper, a vibrational energy harvesting circuit is designed to have a regulated output with small area and MPPT control function to improve the system efficiency.

When MPPT is applied, the input of the DC-DC converter must be stabilized near the MPP. Therefore, if there is no other action, the output of the power converter is an unregulated signal [4], [5]. A method for stabilizing the output is to use a

two-stage power converter structure [7] using an additional DC-DC converter at the output stage, or to use a dual-path structure [8] in which an additional DC-DC converter is connected in parallel to the input stage. However, these structures have the disadvantage that the control circuit is complicated and additional cost is required due to the necessity of an additional DC-DC converter.

In this paper, we propose a structure that uses a PMU (Power Management Unit) at the output stage of the power converter to stabilize the output with simple structure and low cost. Because of the limited size of energy conversion devices applied to micro systems, the energy available through energy harvesting is low and is not sufficient for continuous operation of the system. The active/sleep method is generally used to solve this mismatch [3, 9]. This technique activates the system only when sufficient energy is accumulated, and when the energy is insufficient, the system is turned off (sleep). In this paper, the PMU is designed to implement this technique.

PROPOSED VIBRATIONAL ENERGY HARVESTING CIRCUIT

Fig. 1 shows the block diagram of the proposed vibrational energy harvesting interface circuit with MPPT control. It consists of a vibration device (PZT), an AC-DC converter (full-wave rectifier), an MPPT controller, a DC-DC boost converter and a PMU. The AC signal (V_{PZT}) generated from the PZT device is rectified to a dc signal (V_{FWR}) through the AC-DC converter. The MPPT controller generates a periodic signal MC, and while the MC is '1', the PMOS switch SW1 is opened so that the open circuit voltage (V_{OC}) of the vibration device (including the AC-DC converter) is sampled. While MC is '0', the energy harvested from the PZT device is stored in the storage capacitor C_2. At this time, the voltage V_{DD} becomes equal to the output voltage V_{FWR} of the AC-DC converter and should maintain a value near the MPP in order to harvest the maximum power. To this end, the MPPT controller generates a signal EN for controlling the power switch SW2. While the EN signal is '0', the PMOS switch SW2 is turned on, and the harvested energy is transferred to the input of the DC-DC converter. The output voltage V_{OUT} boosted from the DC-DC converter is converted into a stabilized signal V_L having a duty cycle by the PMU and supplied to the load R_L.

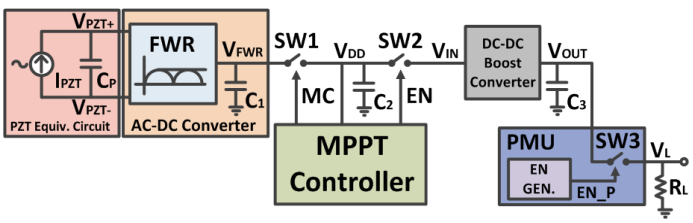

Figure 1: Block diagram of the proposed vibrational energy harvesting circuit.

Vibration Device

The targeted PZT device is the Quick Pack QP20W [11] that can generate 125 µW with an acceleration of 7 m/s^2 at 80 Hz. The PZT device is usually modelled as a sinusoidal current source I_{PZT} in parallel with an internal capacitor C_P as shown in Fig. 1 [8]. The amplitude and frequency of the current source are set to 3 V and 80 Hz, respectively. The internal parallel capacitor is 0.2 µF. The MPP of a PZT device including an AC-DC converter is half of its open-circuit voltage V_{OC}.

AC-DC Converter

Since the output of a PZT device is similar to an ac voltage, an AC-DC converter (ADC) is required to generate a dc voltage. The ADC must have high conversion efficiency in order to transfer the maximum amount of power from the harvester to the load. Conventional passive ADCs using four diode-connected MOSFETs or gate cross-coupled ADCs using two MOS diodes and two MOS switches suffer from diode voltage drop that reduces the available output voltage and thus system efficiency. In this paper an active ADC as shown in Fig. 2 is designed for full-wave rectification without diode voltage drop. The ADC consists of two active diodes and two NMOS switches. The active diode consists of a PMOS switch and a comparator. Fig. 3 shows the results of simulating the P-V and I-V characteristics by connecting the designed ADC to the equivalent PZT model of Fig. 1. The open circuit voltage V_{OC} is 2.97 V, and the voltage at MPP (V_{MPP}) is 1.49 V, which is half of the open circuit voltage. The maximum available power in the MPP is 140.3 µW.

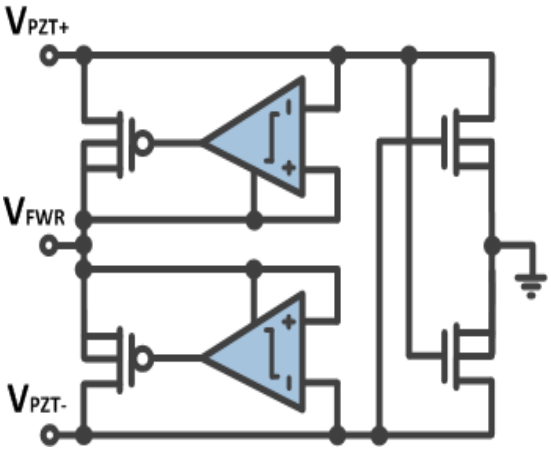

Figure 2: AC-DC converter (ADC).

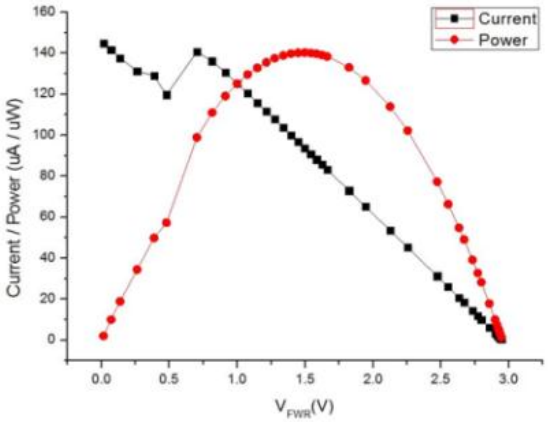

Figure 3: P-V & I-V characteristics of PZT with ADC.

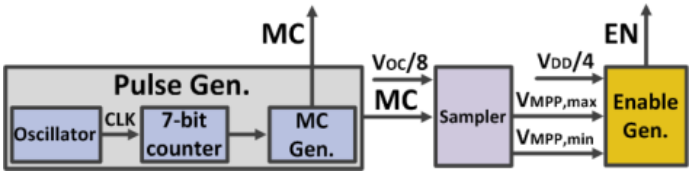

Figure 4: Block diagram of MPPT controller.

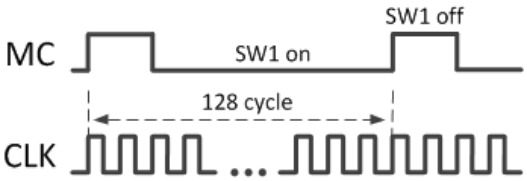

Figure 5: Timing diagram of MPPT clock MC.

MPPT Controller

Fig. 4 shows the block diagram of the MPPT controller that is used to regulate V_{DD} at the MPP and transfer the energy harvested to the DC-DC converter. It consists of a pulse generator, a sampler, and an enable generator. The pulse generator is used to generate a clock pulse (MC) for MPPT control. As shown in Fig. 5 the pulse MC is two cycles long for every 128 cycles of the clock signal (CLK) that is generated using a ring-type oscillator. During this cycle (MC = '1'), the switch SW1 is open, and the V_{MPP} of the energy harvester is sampled by the sampler. In practice, $V_{OC}/8$ is sampled instead of $V_{OC}/2$ (= V_{MPP}) for proper operation of internal circuits. This simple FOC scheme for MPPT control has been proposed in reference [2], where a detailed description of the circuit diagram and operating characteristics of each building block can be found.

DC-DC Boost Converter

The DC-DC boost converter is an asynchronous structure consisting of a single NMOS switch and a schottky diode as shown in Fig. 6. The oscillator is a current-starved ring type structure. The switching frequency is about 2MHz and can be controlled through resistor R_C. Since the boosted output voltage V_{OUT} is transferred to the load through the PMU, it is a simple structure without a feedback path. The operation waveforms of the DC-DC boost converter are shown in Fig. 7. When the output signal EN of the MPPT controller becomes '0' in the overall system of Fig. 1, SW2 becomes 'on' and the input V_{IN} of the DC-DC converter follows V_{DD}. During this interval, the oscillator that is powered from V_{IN} is oscillated, and the output V_{OUT} is boosted. When EN becomes '1', SW2 becomes 'off' and the operation of the DC-DC boost converter is also stopped.

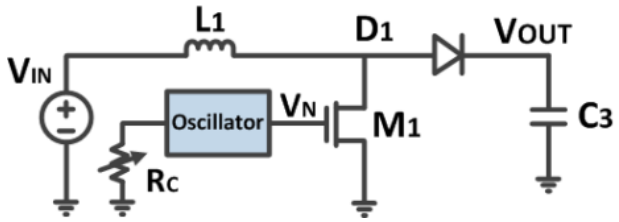

Figure 6: DC-DC boost converter.

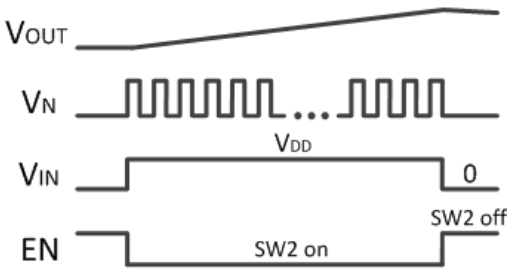

Figure 7: Operation waveforms of DC-DC boost converter.

PMU (Power Management Unit)

The PMU converts the boosted V_{OUT} from the DC-DC boost converter to a stabilized signal having a duty cycle and supplies the stabilized signal to the load. The designed PMU consists of a POR (power on reset), a bias generator, an enable generator, and a PMOS switch, as shown in Fig. 8. When the output voltage V_{OUT} of the DC-DC boost converter increases to 1.3V, the PMU operates by the POR. The bias generator generates the reference voltage and currents necessary for the operation of the enable generator. The structure of the enable generator is shown in Fig. 9, and serves to stabilize the voltage supplied to the load within the range of $V_{L,max}$, and $V_{L,min}$. The values of $V_{L,max}$ and $V_{L,min}$ are determined by R1 to R4, and are set to 3.2 V and 2.8 V respectively in this design. When V_{OUT} increases to reach $V_{L,max}$, SW3 turns on and V_{OUT} is delivered to the load. When V_{OUT} decreases to reach $V_{L,min}$, SW3 turns

off and the power supply to the load is cut off. Therefore, the power supply to the load is active/sleep mode, and the duty cycle varies with the amount of energy harvested from the vibrating device and the magnitude of the load.

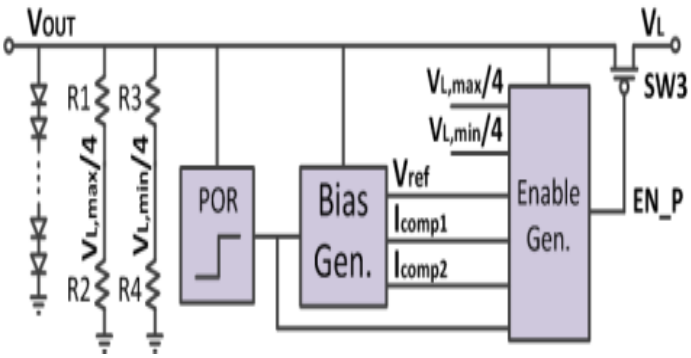

Figure 8: Block diagram of PMU.

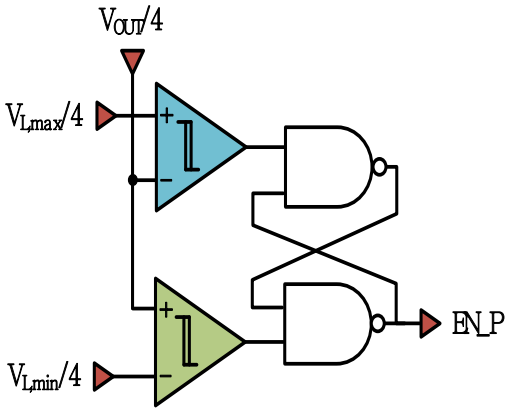

Figure 9: Enable generator.

SIMULATION RESULTS

The designed circuit has been simulated using 0.35-µm CMOS process parameters. Considering that the simulation time becomes too long when simulating with one PZT device, five PZT equivalent circuits are connected in parallel and used as an input. The values of C_1, C_2, C_3, and R_L are set to 2 µF, 100 µF, 100 µF, and 1 kΩ, respectively.

Fig. 10 shows the simulation results of the entire circuit, and Fig. 11 shows the magnified waveforms of the start-up transient and MPPT control. When energy harvesting starts, the MC signal is generated by the MPPT controller, and V_{DD} is stabilized near MPP (1.32 V to 1.52 V) by the MPPT control operation through sampling of the open circuit voltage V_{OC} (= 2.89V).

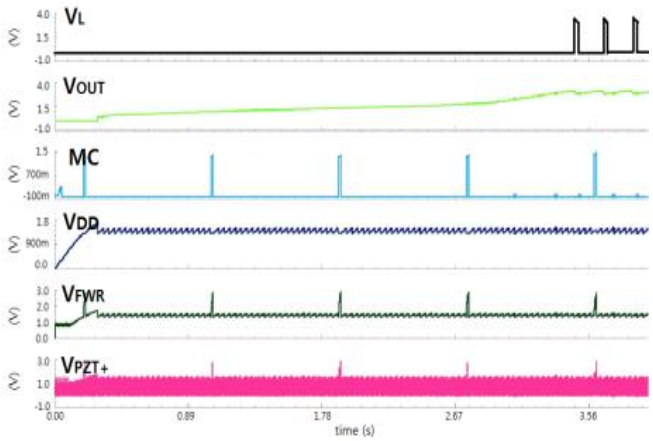

Figure 10: Simulation results of the entire circuit.

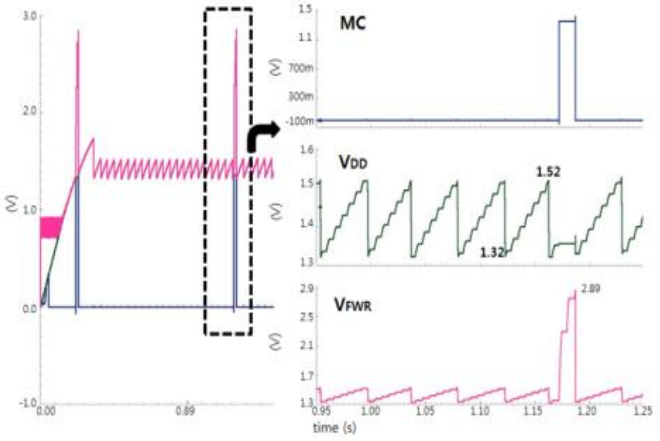

Figure 11: Magnified waveforms of the start-up transient and MPPT control.

Fig. 12 shows the operating waveforms of the DC-DC boost converter. When the output signal EN of the MPPT controller becomes '0', it can be seen that the DC-DC converter operates and the output voltage V_{OUT} increases. When EN is '0', SW2 becomes 'on' and V_{IN} is connected to V_{DD}. During this interval, the oscillator is activated and the output signal V_N drives the power switch M_1 (see Fig. 9). While V_N is 'high', energy builds up through inductor L_1 and switch M_1. While V_N is 'low', the built-up energy is delivered to the output through inductor L_1 and schottky diode D_1, boosting V_{OUT}. It can be seen in Fig. 13 that when V_{OUT} is sufficiently boosted to reach the preset $V_{L,max}$ (3.2V), V_{OUT} is delivered to the load, and when V_{OUT} decreases to the preset $V_{L,min}$ (2.8V), power supply to the load is cut off.

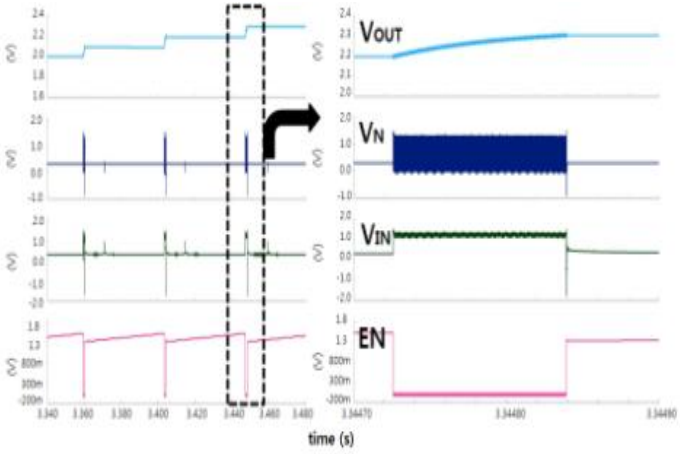

Figure 12: Waveforms of DC-DC boost converter.

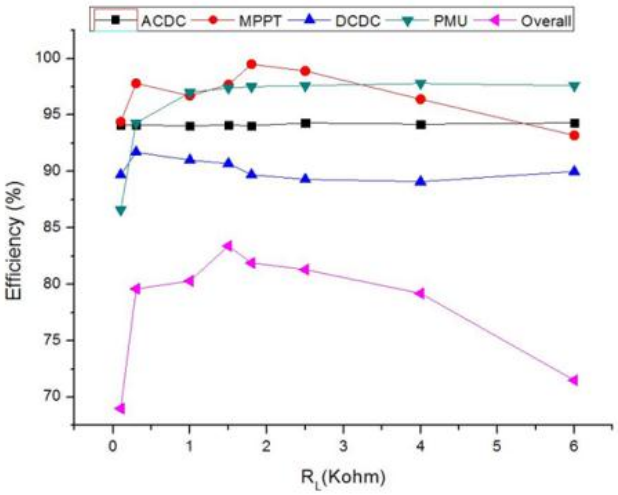

Figure 14: Power efficiency graph.

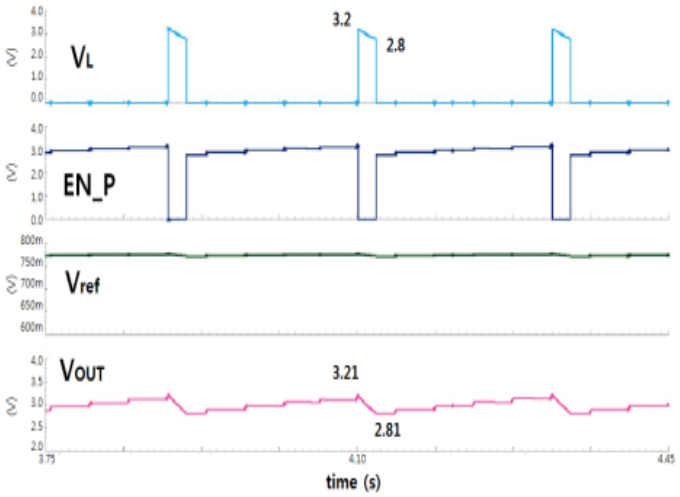

Figure 13: Waveforms of PMU.

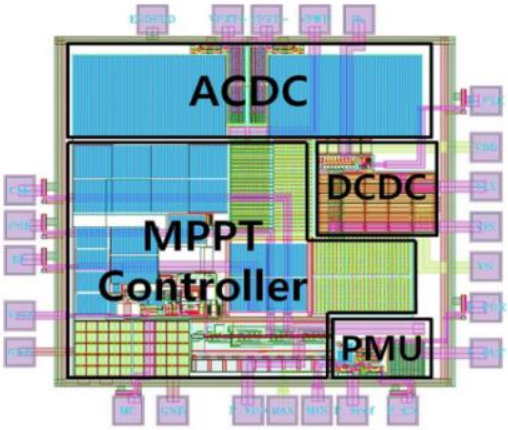

Figure 15: Layout of designed circuit.

Fig. 14 shows the power efficiency graph of each block (AC-DC converter, MPPT controller, DC-DC converter, PMU) and the overall system efficiency graph according to the change of load resistance. The maximum power efficiency of the designed circuit is 83.4% at a load resistance of 1.5 kΩ. The layout of the designed circuit is shown in Fig. 15. The die area excluding the pads is 915 μm × 895 μm.

Table I shows a comparison of the proposed circuit with previously published vibrational energy harvesting designs. The circuit designed in this work shows a high end-to-end power efficiency with a relatively small area and provides a stabilized output. The efficiency of the entire system is improved by applying FOC-type MPPT control, and a stabilized voltage signal in active/sleep mode is supplied to the load by using the PMU.

CONCLUSION

A CMOS interface circuit with MPPT control for vibration energy harvesting has been presented in this paper. The AC-DC converter is implemented using active diodes which are advantageous for high efficiency, and the DC-DC boost converter is implemented using a schottky diode to simplify the control circuit. In order to stabilize the output with a simple structure and a low cost, a structure using the PMU at the output terminal of the DC-DC boost converter is proposed. The proposed circuit is designed with a 0.35-μm CMOS process, and the designed chip area is 915 μm × 895 μm. Simulation results shows that the maximum end-to-end power efficiency of the designed circuit is 83.4%. The vibrational energy harvesting circuit designed in this work can be applied to various applications where a relatively low duty-cycle operation is required, such as structural or environmental monitoring systems.

Table 1: Proposed dual-input energy harvesting circuit using vibration and thermoelectric energy.

Parameters	**[3]**	**[4]**	**[5]**	**[6]**	**This work**
Process	0.35μm CMOS	Off-chip	0.35μm BCD	0.5μm CMOS	0.35μm CMOS
MPPT algorithm	FOC	P&O	FOC	None	FOC
Operation mode	active/sleep	continuous	continuous	continuous	active/sleep
AC-DC type	1-stage AD	N/A	1-stage AD	2-stage AD	1-stage AD
DC-DC type	None	Buck-Boost	Buck-Boost	Boost	Boost
Frequency (Hz)	~200	44~53	~200	1~100k	~200
Input voltage (Voc)	~6.5V	3~25V	1~7V	1~3V	2.5~5V
Output voltage	~6.5V	3V~	1~8V	3V (Regulated)	3V (Regulated)
Maximum Power Efficiency (%)	None	76 (just DC-DC)	80 (just DC-DC)	60 (end-to-end)	83.4 (end-to-end)
Maximum MPPT efficiency (%)	98.3	97	99	None	99
Voc sensing time	2 cycles	N/A	1 cycle	None	2 cycles
Chip area (mm^2)	1.68 (w/ pads)	None	5.52 (w/ pads)	0.026 (AC-DC) 0.117 (DC-DC)	0.82

<Note> FOC: Fractional Open-Circuit, P&O: Perturbation & Observation, AD: Active Diode

ACKNOWLEDGEMENT

The author would like to thank Min-Jae Yang for simulation support and this work was partially supported by IDEC.

REFERENCES

[1] Kuoa, Y. C., Huanga, Y. M., and Liub, L. J., 2014, "Integrated circuit and system design for renewable energy inverters," International Journal of Electrical Power & Energy Systems, 64, pp. 50-57.

[2] Yoon, E.-J., and Yu, C.-G., 2016, "Auto-Switching Energy Harvesting Circuit for Low-Power Sensing Systems," International Journal of Applied Engineering Research, 11(8), pp. 5856-5862.

[3] Lu, C., Tsui, C.-Y., and Ki, W.-H., 2011, "Vibration energy scavenging system with maximum power tracking for micropower applications," IEEE Trans. on VLSI Systems, 19(11), pp. 2109-2119.

[4] Kong, N., and Ha, D. S., 2012, "Low-Power Design of a Self-powered Piezoeletric Energy Harvesting System With Maximum Power Point Tracking," IEEE Trans. on Power Electronics, 27(5), pp. 2298-2308.

[5] Shim, M., et al., 2015, "Self-Powered 30 μW to 10 mW Piezoelectric Energy Harvesting System With 9.09 ms/V Maximum Power Point Tracking Time," IEEE J. Solid-State Circuits, 50(10), pp. 1-13.

[6] Rao. Y., and Arnold, D. P., 2011, "An Input-powered Vibrational Energy Harvesting Interface Circuit with Zero Standby Power," IEEE Trans. on Power Electronics, 26(12), pp. 3524-3533.

[7] Ramadass, Y. K. and Chandrakasan, A. P., 2011, "A battery-less thermoelectric energy harvesting interface circuit with 35 mV startup voltage," IEEE J. Solid-State Circuits, 46(1), pp. 333–341.

[8] Bandyopadhyay, S., and Chandrakasan, A. P., 2012, "Platform Architecture for Solar, Thermal, and Vibration Energy Combining With MPPT and Single Inductor," IEEE J. Solid-State Circuits, 47(9), pp. 2199-2215.

[9] Colomer-Farrarons, J., Miribel-Catala, P., Saiz-Vela, A., Puig-Vidal, M., and Samitier, J., 2008, "Power-conditioning circuitry for a self-powered system based on micro PZT generators in a 0.13 μm low-voltage low-power technology," IEEE Trans. on Industrial Electronics, 55(9), pp. 3249–3257.

[10] Seeman, M. D., Sanders, S. R., and Rabaey, J. M., 2008, "An Ultra-Low-Power Power Management IC for Energy-Scavenged Wireless Sensor Nodes," in Proc. 2008 PESC, pp. 925-931.

[11] QP20W, Mouser Electronics [Online]. Available: http://www.mouser.com/.